PHOSPHODIESTERASE 2A FORMS A COMPLEX WITH THE CO-CHAPERONE XAP2 AND REGULATES NUCLEAR TRANSLOCATION OF THE ARYL HYDROCARBON RECEPTOR

Simone Kobe de Oliveira[§¶], Meike Hoffmeister[§], Stepan Gambaryan[‡||], Werner Müller-Esterl[§], Jorge A. Guimaraes[¶] and Albert P. Smolenski[§]**

From the [§]Institute of Biochemistry II, University of Frankfurt Medical School, Frankfurt, Germany;

[¶]Biotechnology Center, UFRGS, Porto Alegre, Brazil

[‡]Institute of Clinical Biochemistry and Pathobiochemistry, University of Würzburg, Germany;

[||]Sechenov Institute of Evolutionary Physiology and Biochemistry, Russian Academy of Sciences, St Petersburg, Russia

Running title: PDE2A interacts with XAP2

**Address correspondence to: Albert Smolenski, Institute of Biochemistry II, University of Frankfurt Medical School, Theodor-Stern-Kai 7, 60590 Frankfurt, Germany; Tel. +49-69-6301-5569; Fax. +49-69-6301-5577; E-Mail: smolenski@biochem2.de.

Phosphodiesterase type 2A (PDE2A) hydrolyzes cyclic nucleotides cAMP and cGMP thus efficiently controlling cNMP-dependent signaling pathways. PDE2A is composed of an N-terminal region, two regulatory GAF domains and a catalytic domain. Cyclic nucleotide hydrolysis is known to be activated by cGMP binding to GAF-B, however, other mechanisms may operate to fine-tune local cyclic nucleotide levels. In a yeast-two-hybrid screening we identified XAP2, a crucial component of the aryl hydrocarbon receptor (AhR) complex, as a major PDE2A-interacting protein. We mapped the XAP2 binding site to the GAF-B domain of PDE2A. PDE assays with purified proteins showed that XAP2 binding does not change the enzymatic activity of PDE2A. To analyze if PDE2A could affect the function of XAP2 we studied nuclear translocation of AhR, i.e. the master transcription factor controlling the expression of multiple detoxification genes. Notably, regulation of AhR target gene expression is initiated by tetrachlorodibenzodioxin (TCDD) binding to AhR and by a poorly understood cAMP-dependent pathway, followed by the translocation of AhR from the cytosol into the nucleus. Binding of PDE2A to XAP2 inhibited TCDD- and cAMP-induced nuclear translocation of AhR in Hepa1c1c7 hepatocytes. Furthermore, PDE2A attenuated TCDD-induced transcription in reporter gene assays. We conclude that XAP2 targets PDE2A to the AhR complex thereby restricting AhR mobility, possibly by a local reduction of cAMP levels. Our results provide first insights into the elusive cAMP-dependent regulation of AhR.

Cyclic nucleotide phosphodiesterases (PDEs) catalyze the hydrolysis of cAMP and/or cGMP. In conjunction with adenylyl and guanylyl cyclases PDEs regulate the amplitude and duration of cell signaling events mediated by cyclic nucleotides. In this context PDEs are involved in a broad range of biological responses such as cardiac contractility, platelet aggregation, lipolysis, glycogenolysis, smooth muscle contraction, ion channel conductance, and apoptosis (1). Sequence analyses suggest that 11 different families of mammalian PDEs exist and most of these families contain more than one gene product. Furthermore, many of these genes can be alternatively spliced in a tissue specific manner to give rise to several different isoenzymes with altered regulatory properties, subcellular localization and different substrate specificities. The distinct cellular localization and biophysical characteristics of the various PDEs suggest that each PDE is individually regulated and plays distinct roles in specific physiological processes (2).

PDE2A is activated by cGMP and degrades both, cAMP and cGMP. PDE2A is highly expressed in the brain and heart, but it is also found in lung, kidney, liver and adrenal gland (3). One of the first specific functions attributed to PDE2A was the regulation of aldosterone production in adrenal zona glomerulosa cells (4). Recently, PDE2A was found to attenuate spatially confined pools of cAMP in cardiac myocytes, thereby affecting contractile function (5). Moreover, PDE2A appears to increase permeability of endothelial layers and thus to impair endothelial barrier function (6). PDE2A is composed of an N-terminal domain of unknown function, two

central GAF domains (A and B) and a C-terminal catalytic domain (7,8). Structural analysis of the PDE2A GAF domains revealed that only the GAF-B domain is involved in cGMP binding, whereas the N-terminal GAF-A domain is required for dimerization (7).

Here we report that PDE2A associates with XAP2, a member of the immunophilin protein family. XAP2 (also known as ARA9 or AIP) is a 38-kDa protein that was initially identified as a protein binding to the hepatitis B virus X protein (9) and in parallel also as binding partner of the aryl hydrocarbon receptor (AhR) (10-12). XAP2 shares sequence identity with FKBP52, an immunophilin of the FK506 binding proteins and an established component of the glucocorticoid receptor complex. Although XAP2 contains an immunophilin homology domain within its N-terminal region, no binding to immunosuppressant drugs was found (10). The C-terminus of XAP2 contains multiple tetratricopeptide repeat (TPR) motifs that mediate protein-protein interactions (13) and XAP2 has been shown to engage in a multiprotein complex together with a dimer of Hsp90, p23 and AhR (14,15). AhR is a ligand-activated transcription factor and belongs to the basic helix-loop-helix Per/ARNT/Sim family of proteins (16,17). The activity of the AhR is regulated by structurally diverse xenobiotics such as the high affinity ligand 2,3,7,8-tetrachlorodibenzo-*p*-dioxin (TCDD) (18). Upon ligand binding, the AhR translocates to the nucleus and dimerizes with the structurally related protein ARNT. The resultant complex interacts with enhancer elements upstream of target promoters and drives the transcription of a host of xenobiotic metabolizing enzymes (19). Recently, cAMP has been described as a mediator of AhR translocation, acting as a repressor rather than an activator of AhR-dependent gene expression (20), however the underlying molecular pathways have remained elusive. Here we identify a functional interaction between PDE2A and AhR pathways that is mediated by XAP2, an essential component of the AhR complex, providing a direct link between cAMP- and TCDD-dependent pathways.

EXPERIMENTAL PROCEDURES

Materials. The full length PDE2A cDNA (Clone IRAKp961N0275Q2, GenBank™ accession number BC040974) was obtained from RZPD (Berlin, Germany). 8-Br-cAMP and db-cAMP were from Biolog (Bremen, Germany), 2,3,7,8-tetrachlorodibenzo-p-dioxin (TCDD) and forskolin were from Sigma (Taufkirchen, Germany). HRP-coupled goat-anti-rabbit and goat-anti-mouse were from Dianova (Hamburg, Germany).

Two-hybrid screening. The complete PDE2A cDNA was cloned into the SfiI and SalI sites of the pGBKT7 vector (Clontech, Takara Bio Europe, St-Germain-en-Laye, France). This construct encodes a fusion between the amino-terminal end of PDE2A and the Gal4 DNA-binding domain (bait). The screen was performed with a human brain two-hybrid cDNA library (Matchmaker Two-Hybrid System 3, Clontech) cloned into the XhoI and EcoRI sites of the pACT2 vector and expressing proteins as fusions with the Gal4 protein activation domain. This library was transformed into *S. serevisiae* strain AH109 expressing the PDE2A bait construct. Positive clones were initially selected for growth in the absence of adenine, histidine, leucine and tryptophane. Library plasmid DNA was isolated from the positives clones and re-transformed into yeast strain AH109 containing the bait and the re-transformed positives clones were further assayed for the PDE2A interaction.

Cell culture and transfection. COS-1 and HeLa cells were cultured in Dulbecco's modified Eagle's medium (DMEM) supplemented with 10% fetal calf serum (PAA, Pasching, Austria) and 1% penicillin/streptomycin (PAA). Transient transfections of COS-1 cells were performed with DEAE-dextran. Briefly, $6x10^5$ cells were seeded per 10 cm dish. On the following day, cells were washed with PBS, and expression plasmids were applied in 5.7 ml serum-free DMEM mixed with 300 µl of DEAE-dextran (1 mg/ml stock) and 12 µl chloroquine (100mM stock). After incubation for 2 hours, the transfection mixture was removed and cells were cultured in DMEM with 10% FCS for 48 hours prior to harvesting. HeLa cells were transiently transfected using Metafectene (Biontex, Martinsried, Germany) according to the manufacturer's instructions. The mouse hepatoma cell line (Hepa1c1c7), a kind gift from Barbara Oesch-Bartlomowicz (University of Mainz, Mainz, Germany), was propagated in α-MEM (Invitrogen, Karlsruhe, Germany) supplemented with 10% FCS and 1% penicillin/streptomycin and transfections were performed with Fugene 6 (Roche Diagnostics, Mannheim, Germany) according to the manufacturer's instructions. All cells were maintained as monolayers in an atmosphere of

5% CO_2 and 95% air under saturating humidity at 37°C.

Generation of mammalian cell expression constructs. The PDE2A cDNA was cloned into the EcoRV and HindIII sites of the pSG8 vector (21) to generate a fusion construct with a N-terminal vesicular stomatitis virus glycoprotein epitope (VSV) sequence. A similar expression plasmid was generated to encode only the GAF-B domain of PDE2A. The circular site-direct mutagenesis method was used to introduce stop codons into the full length PDE2A cDNA in pSG8 to obtain constructs expressing the N-terminus (N-PDE2A), whole GAF A and GAF A/B domains N-terminally fused to a VSV tag. The complete XAP2 cDNA (GenBank™ accession number U31913) was cloned into the HindIII and XhoI sites of pcDNA4/TO (Invitrogen) with a FLAG epitope-tag immediately downstream of the last codon of the XAP2 cDNA and into pcDNA3.1-myc containing a myc-epitope at the N-terminus. The FLAG-AhR (human) construct was a kind gift of Gary H. Perdew (Pennsylvania State University) and the p1646p1Luc3 reporter plasmid was provided by Alvaro Puga (University of Cincinnati).

Pull-down experiments. The XAP2 cDNA was cloned into the SmaI and NotI site of the pGEX4T-3 vector (GE Healthcare, Freiburg, Germany) to generate a fusion between glutathione *S*-transferase (GST) and the amino-terminus of XAP2. Additonally, XAP2 truncated constructs encoding GST fusions to the amino-terminal (amino-acids 1-169; to create GST-N-XAP2) or carboxy-terminal (amino-acids 170-330; to create GST-C-XAP2) regions of XAP2 were generated. *E. coli* BL21(DE3) were transformed with these constructs and protein expression was induced with 0.4 mM of isopropyl-beta-D-thiogalactopyranoside (IPTG) for 3 hours at 37°C. The recombinant proteins were purified with glutathione 4B-Sepharose beads (GE Healthcare). COS-1 cells transfected with expression constructs for VSV-PDE2A were lysed by scraping in 500 µl of ice-cold lysis buffer (50 mM Tris-HCl, pH 7.5, 150 mM NaCl, 1% Triton X-100, 5 mM $MgCl_2$, including the following protease inhibitors: 1.12 mM DTT, 50 µM chloroquine, 2 µg/ml aprotinin, 1 µg/ml leupeptin and 1 µg/ml PMSF). Lysates were centrifuged for 20 min at 13,000 x *g* and 4 °C and the cleared supernatants were collected. GST pull-down experiments were carried out by incubating 10 µl of glutathione sepharose beads saturated with GST-XAP2, GST-N-XAP2 or GST-C-XAP2 with 500 µl of cleared COS-1 cell lysates for 4 hours at 4°C. Beads were washed 5 times with lysis buffer before adding 10 µl 3x SDS sample buffer and boiling for 5 minutes. Proteins were separated on 10% SDS-PAA gels and identified by immunoblotting with anti-VSV antibody (clone P5D4 obtained from Sigma). For activity assays the GST fusion proteins were eluted from the beads with 800 µl of 10 mM reduced L-glutathione (Sigma)

Immunoprecipitation. Cells were harvested and lysed by scraping in 500 µl of ice-cold lysis buffer. Lysates were centrifuged for 20 min at 13,000 x *g* and 4 °C and supernatants were used to precipitate XAP2-FLAG using 5 µl of anti-FLAG M2 Affinity Gel (Sigma) at 4 °C for 2 h. Immunoprecipitates were washed four times with 1 ml of lysis buffer and coprecipitated VSV-PDE2A was detected by immunoblotting with anti-VSV antibody. For immunoprecipitation of endogenous proteins male CD rats were anaesthesized by ether and decapitated. Brain tissue was immediately isolated and homogenized in immunoprecipitation (IP) buffer (50 mM Tris, pH 8, 150 mM NaCl, 1 mM EDTA, 1% IGEPAL, 0.1 mM PMSF and protease inhibitors complete Mini (Roche Diagnostics)). Insoluble material was removed and supernatants were incubated with either rabbit IgG as control, XAP2 antibody (Abcam, Cambridge, UK), or PDE2A antibody (FabGennix Inc., Frisco, TX) for 1 h at 4°C. Then protein G (for XAP2 sample) or protein A (for control and PDE2A sample) Sepharose 4B fast flow beads (GE Healthcare) were added for 1 h. Immunecomplexes were washed 3 times with IP buffer and twice with PBS and precipitated proteins were detected by immunoblotting.

PDE2A activity assay. COS-1 cells (5 x 10 cm dishes) transfected with pSG8-PDE2A or with empty pSG8 vector (mock) were harvested in 1 ml lysis buffer and immunoprecipitated with 10 µl of mouse anti-VSV antibody for 2 hours followed by incubation with 200 µl protein A/G-PLUS agarose beads (Santa Cruz Biotechnology, Heidelberg, Germany) for 1 hour. Beads were washed 4 times with 20 mM Tris-HCl buffer (pH 7.5). Catalytic activity of PDE2A was assayed using the PDElight™ kit (Cambrex Bio Science, Verviers, Belgium) according to the manufacturer's instructions. Briefly, PDE2A induced hydrolysis of cAMP generates AMP which is phosphorylated to ATP. ATP is the energy source for the luciferin/luciferase oxidation reaction resulting in light emission. The emitted light is

directly proportional to the level of AMP present in the reaction which is a function of PDE activity. 5 µl of PDE2A beads (approximately 2.5 nM final concentration) were incubated with 125 nM of each GST fusion protein: GST-XAP2, GST-N-XAP2, GST-C-XAP2 or GST in 20 mM Tris-HCl, pH 7.5, 5 mM $MgCl_2$ buffer for 10 minutes at room temperature, followed by addition of 25 µM cAMP and incubation for 1 hour at 30°C. The reaction was stopped and luminescence was measured using a 96-well microplate reader Wallac Victor^3 1420 Multilabel Counter (Perkin Elmer, USA).

AhR translocation and co-localization experiments. 0.15 x 10^5 Hepa1c1c7 cells were seeded per chamber (1.8 cm^2) of a 4-chamber slide, allowed to grow for 48 hours and transfected without or with the expression vector for VSV-tagged PDE2A. 24 hours posttransfection, cells were incubated with 2 mM 8-Br-cAMP, 20 µM forskolin or 5 nM 2,3,7,8-tetrachlorodibenzo-p-dioxin (TCDD) for 1h at 37 °C, fixed with 3.7% paraformaldehyde and permeabilized with 0.2% Triton-X-100 in PBS. Then cells were incubated with anti-AhR M20 (1:50, Santa Cruz Biotechnology) and anti-VSV P5D4 (Sigma) for 2 hours, followed by incubation with Cy3-conjugated anti-goat IgG and Cy2-conjugated anti-mouse IgG (Jackson ImmunoResearch, Newmarket, England) for 1 hour. For co-localization experiments, HeLa and Hepa1c1c7 cells were transfected with pSG8-VSV-PDE2A and pcDNA3.1-myc-XAP2. After 1 day cells were fixed and permeabilized as described above and stained with anti-VSV and anti-myc (Santa Cruz Biotechnology) primary antibodies for 1 hour at 37°C followed by staining with Cy-conjugated antibodies as described. Chamber slides were mounted in GEL/mount (Biomeda, Foster City, CA) and cells were analyzed with a Zeiss LSM 510 confocal laser scanning microscope equipped with a Plan-Apochromat 63 /1.4 oil DIC objective lens and LSM 510 META software (Carl Zeiss, Göttingen, Germany). For quantitative evaluation of PDE2A effects on AhR translocation 70 to 200 cells from at least three independent experiments were analyzed. Cells exhibiting cytosolic as well as nuclear staining of AhR were assigned to the "spread" group, whereas cells having a stronger or exclusive nuclear AhR staining were assigned "nuclear".

Reporter assay. 0.3 x 10^4 Hepa1c1c7 cells were seeded per well of a 96 well plate. After 48 hours cells were transfected with 10 ng of pRL-SV40 (Promega GmbH, Mannheim, Germany), 225 ng of either pGL3-Basic (Promega) or p1646p1Luc3 and 75 ng of either pSG8 or PDE-pSG8. 24 hours posttransfection, cells were stimulated with 5 nM TCDD for 4 h. The luminescence was measured using the Dual-Luciferase Assay System (Promega) according to the manufacturer´s instructions. The relative light units (RLU) were normalized to the expression of the *Renilla* luciferase. Data were collected from 4 independent experiments performed in quadruplicate. To verify expression of PDE, lysed cells were collected after each experiment, proteins were precipitated using aceton, solubilized in SDS sample buffer and analyzed by SDS-PAGE and immunoblotting.

RESULTS

Yeast two-hybrid screening for PDE2A interaction partners and identification of XAP2

To identify proteins that interact with PDE2A we performed a yeast two-hybrid screen. We used human PDE2A as bait and a human adult brain cDNA library as prey. A total of 236 clones were isolated and rescreened by retransformation and X-Gal staining. The remaining 141 positive clones were sequenced, cDNA artifacts and extracellular proteins were excluded, and 6 out of 25 putative PDE2A binding partners were selected for further analysis. We expressed the candidate proteins in *E.coli* as GST fusion proteins coupled to the C-terminus of GST. Pull-down assays were performed using lysates from mammalian COS-1 cells transfected with PDE2A expression vectors. Two of these GST fusion proteins bound to PDE2A and one of these was XAP2, a 330 amino-acid protein of the immunophilin family (Fig. 1A and B). For control unfused GST was used revealing that GST alone does not pull-down PDE2A (Fig. 1A and B).

PDE2A interacts with XAP2 in intact mammalian cells

To confirm that PDE2A and XAP2 bind to each other in intact cells we performed co-immunoprecipitation experiments. For this purpose, the VSV epitope was fused to the N-terminus of PDE2A, and XAP2 was C-terminally tagged with a FLAG epitope. Both proteins were expressed in COS-1 cells, either alone or in combination, and XAP2 was precipitated using anti-FLAG. Analysis of the precipitates by immunoblotting with anti-VSV revealed the presence of PDE2A only in precipitates from

cells expressing both PDE2A and XAP2 (Fig. 1C). We confirmed the binding in a reverse experiment using anti-VSV to precipitate PDE2A followed by blotting for XAP2 with anti-FLAG (data not shown). To verify the interaction of PDE2A and XAP2 at the level of endogenous proteins we performed co-immunoprecipitation experiments in lysates prepared from brain tissue. Analysis of the total lysate by immunoblotting confirmed the expression of both, PDE and XAP2 (Fig. 1D, first lane). Using a specific antibody against XAP2 we could precipitate endogenous XAP2. Immunoblotting of the XAP2 precipitates with a PDE2A antibody revealed the presence of endogenous PDE2A (Fig. 1D, third lane). In a reverse experiment using anti-PDE2A for immunoprecipitation we could detect XAP2 in the precipitates by immunoblotting. No unspecific binding of the proteins occured in a control experiment using non-specific IgG (Fig. 1D, second lane). These results clearly confirm the interaction of PDE2A with XAP2.

PDE2A and XAP2 colocalize in cells

Next we investigated the subcellular localizations of PDE2A and XAP2 by immunofluorescence. Since our antibodies to FLAG generated a strong unspecific background in immunofluorescence stainings we created a myc-tagged construct of XAP2. HeLa cells were cotransfected with VSV-tagged PDE2A and myc-tagged XAP2 followed by fixation and immunostaining with tag-specific primary antibodies and labeled secondary antibodies. Both proteins localized to the cytosol in a reticular pattern (Fig. 2). Occasionally, staining of regions close to the plasma membrane could be observed. The subcellular distributions of PDE2A and XAP2 were similar and the overlay revealed an extensive colocalization of the two proteins (Fig. 2C). A similar result was obtained after transfection and staining of PDE2A and XAP2 in mouse Hepa1c1c7 cells (data not shown). To exclude cross-reactivity of secondary antibodies we stained transfected cells with a single primary antibody at a time, followed by both secondary antibodies. Only the appropriate secondary antibody bound to its target primary antibody confirming specificity of the probes (data not shown). Together these experiments show that PDE2A and XAP2 may interact *in vitro* and in intact cells.

The GAF-B domain of PDE2A mediates binding to XAP2

To determine the domain of PDE2A involved in binding to XAP2 we generated various constructs of PDE2A containing either the N-terminus of PDE2A (N-PDE2A), the N-terminus and the GAF-A domain (GAF-A), the N-terminus and both GAF domains (GAF-A/B), or the GAF-B domain alone (GAF-B) (Fig. 3A). All PDE2A constructs were N-terminally fused to VSV. The constructs were transfected into COS-1 cells and full-length GST-XAP2, as well as GST alone as control were used to precipitate the various PDE2A constructs from cell lysates. Full-length PDE2A, GAF-A/B and the GAF-B domain alone readily bound to XAP2, while N-PDE2A and GAF-A alone failed to bind XAP2 (Fig. 3B). We conclude that the GAF-B domain of PDE2A is necessary and sufficient to mediate interaction with XAP2.

The C-terminus of XAP2 is required for binding to PDE2A

XAP2 is composed of a N-terminal immunophilin homology domain and a TPR domain at the C-terminus (Fig. 4A). TPR domains are known to mediate protein/protein interactions (10). To identify the region involved in the binding of XAP2 to PDE2A we constructed two GST-fusion proteins containing the N-terminal half of XAP2 (N-XAP2) or its C-terminus, including the TPR domain (C-XAP2). For control GST alone and full-length GST-XAP2 were used. Proteins were expressed in *E.coli* (Fig. 4B), affinity-purified and used to pull-down PDE2A from lysates of COS-1 cells transfected with the VSV-tagged full-length PDE2A construct. Figure 4B demonstrates that all constructs migrated at their expected molecular weight. Full-length XAP2 and C-XAP2 bound to PDE2A, whereas GST alone and N-XAP2 did not (Fig. 4C). These data suggest that XAP2 interacts with PDE2A via its C-terminal domain, most likely via its TPR motif.

Binding of XAP2 does not change the catalytic activity of PDE2A

To monitor for functional consequences of XAP2 binding to PDE2A we measured the catalytic activity of PDE2A *in vitro* in the presence or absence of XAP2. For this purpose we expressed VSV-tagged wild-type PDE2A in COS-1 cells. PDE2A was purified from cellular lysates by immunoprecipitation using anti-VSV, and the purity of the preparation was assessed (Fig. 5A). Full-length XAP2, as well as N-XAP2 and C-XAP2 were expressed as GST fusion proteins in *E.coli*. To test the specificity of our PDE assay and to rule out unspecific effects by endogenous esterases from COS-1 cells we tested PDE

activity in various cell lysates. A 20-fold increase in PDE activity was observed in preparations isolated from PDE2A-expressing COS-1 cells over mock-transfected COS-1 cells or buffer alone (Fig. 5B). Addition of cGMP to the assay did not increase the catalytic activity of PDE2A (data not shown), indicating that the enzyme was fully saturated with cGMP due to the high cytosolic cGMP concentration in COS-1 cells (approximately 10 μM (22)) and the high binding affinity of PDE2A for cGMP (IC_{50} = 22 nM (8)). Next, we measured PDE activities in the absence and presence of XAP2. To mimic high local concentrations of XAP2 in subcellular compartments, we used a 50-fold molar excess of XAP2 constructs (125 nM) over PDE2A (2.5 nM). Neither full-length nor N- or C-XAP2 constructs significantly changed the catalytic activity of PDE2A (Fig. 5B). We conclude that XAP2 binds to PDE2A without affecting its catalytic capacity. By implication we infer that XAP2 does not interfere with cGMP binding, though this has not been tested experimentally.

PDE2A inhibits nuclear translocation of the AhR complex in Hepa1c1c7 cells

XAP2 is a well established component of the AhR complex (10-12). Binding of ligands such as TCDD triggers translocation of the complex to the nucleus. Translocation is followed by a reorganization of the protein complex, recruitment of the ARNT protein, and finally docking to target genes. Because cAMP has been shown to induce nuclear translocation of the AhR (20), we wondered whether PDE2A affects TCDD-induced nuclear translocation of the AhR. For these experiments we used Hepa1c1c7 cells which are known to express AhR and XAP2 endogenously (12). After transfection of PDE2A cDNA cells were incubated for 1 h with 5 nM TCDD and the subcellular localization of AhR was monitored by indirect immunofluorescence. Untreated cells exhibited a diffuse localization of AhR all over the cytosol and occasionally involving the nucleus. In some untreated cells expressing PDE2A a reduced nuclear staining of AhR was observed (Fig. 6B and C). As expected, TCDD induced a strong enrichment of AhR in the nucleus, while the cytosol appeared largely devoid of AhR (Fig. 6, A versus D). In PDE2A expressing cells (Fig. 6E and F) AhR staining remained diffuse without significant nuclear accumulation of AhR in most cells. Next, we tested the effects of PDE2A on cAMP-mediated nuclear translocation of the AhR. In line with previous findings (20) forskolin, an activator of adenylyl cyclase, and cAMP analog 8-Br-cAMP induced nuclear translocation of AhR (Fig. 6G and J). Compared to TCDD, the effects induced by cAMP were not so drastic and some degree of cytosolic AhR staining always remained after cAMP treatments, in accordance with previous observations (20). In PDE2A expressing cells cAMP-induced nuclear translocation of AhR was strongly reduced (Fig. 6H and I versus 6G and 6K and L versus 6J). Quantitative evaluation of these experiments showed that TCDD, forskolin and 8-Br-cAMP induced nuclear translocation of AhR in approximately 80% (78.6% to 82.6%) of the cells (Table 1). In PDE2A expressing cells we found that the TCDD-induced nuclear translocation of AhR was substantially reduced to 43%. Nuclear translocation induced by forskolin or 8-Br-cAMP in PDE2A expressing cells was down to 23.5 % and 18% respectively, of control (Table 1). Thus the presence of PDE2A significantly interferes with the nucleo-cytosolic distribution pattern of AhR.

PDE2A attenuates gene expression induced by TCDD in Hepa1c1c7 cells

To test if the reduced nuclear translocation of the AhR interfered with its function in the nucleus we performed reporter gene assays. We transfected a reporter construct containing the cytochrome P450 (Cyp1a1) natural promoter, including 6 dioxin responsive elements, fused to luciferase into Hepa1c1c7 cells. As shown before (20), treatment with TCDD increased the expression of the reporter gene (Fig. 7). Expression of PDE2A resulted in a moderate but significant reduction of TCDD-dependent induction of the reporter (Fig. 7). In cells expressing a control plasmid lacking the Cyp1a1 promoter no significant changes in reporter gene activity were observed (Fig. 7). We conclude that inhibition of nuclear translocation of AhR by PDE2A correlates with reduced AhR function.

DISCUSSION

PDE2A is one of the major phosphodiesterases that regulates cyclic nucleotide levels through positive feed-back mechanisms, i.e. increasing cGMP concentrations stimulate phosphodiesterase activity thus keeping intracellular cyclic nucleotide levels in tight check. Accumulating evidence suggests that local cGMP levels may be important to drive cyclic nucleotide-dependent signaling cascades in distinct subcellular compartments, and therefore it has been speculated that effector proteins

binding to PDE2A may impact on various cGMP-dependent processes. For instance, Bentley et al. showed by a co-immunoprecipitation approach that various phosphoproteins can bind to epitope-tagged PDE2A in PC12 cells, however, the identity of these phosphoproteins was not disclosed (23). Here we have identified XAP2 as a novel binding partner of PDE2A, and we provide evidence for a new role of PDE2A in the AhR pathway. Other binding partners for PDE2A may well exist, as revealed by the results of our yeast two-hybrid screening, however, these potential interactors await further characterization.

The GAF-B domain of PDE2A mediates XAP2 binding

PDE2A contains regulatory segments consisting of two GAF domains A and B. cGMP binds exclusively to GAF-B and enhances allosterically its catalytic activity, accounting for numerous physiological consequences *in vivo* (7,8). N-terminal tandem GAF domains are present in 5 out of 11 mammalian PDE families. The ligand for the GAF domains of PDEs 2, 5, 6 and 11 is cGMP, whereas cAMP binds to PDE10 (24). Binding of proteins to the GAF domains of PDEs has not been reported to date. Our biochemical analyses clearly show that the GAF-B domain is necessary and sufficient to mediate binding of XAP2 to PDE2A.

Interestingly, Bolger et al. have recently identified XAP2 as a specific interaction partner for the cAMP-specific PDE4A5 (25). In their study XAP2 binding was specifically restricted to the A5 isoform of PDE4, whereas PDE4 isoforms A1, A8, B2, B3, D3, D4 and D5 did not bind XAP2. A careful mapping study revealed that the N-terminal region of PDE4A5 holding an EELD motif in the upstream conserved region-2 exposes the major binding site of XAP2. This segment has no apparent similarity to GAF-B of PDE2A, suggesting different modes of XAP2 binding among PDE isotypes.

The C-terminal part of XAP2 docks to PDE2A

Our mapping studies revealed that the C-terminus of XAP2 is solely responsible for PDE2A binding. This C-terminal portion of XAP2 holds a TPR domain known to mediate protein-protein interactions critical for the assembly of multi-protein complexes (13,26). At present, the relationship between the number and arrangement of TPR repeats and their affinity and specificity for target proteins such as the various PDE subtypes is still unclear. The TPR domain of XAP2 has also been implicated in the binding of Hsp90 (25,27,28). Our preliminary experiments indicate that XAP2 can bind simultaneously to PDE2A and Hsp90 (data not shown), however, the fact that Hsp90 binds to both, XAP2 and PDE2A, makes it difficult to discriminate between the various ternary complexes.

Role of XAP2 for PDE function

To test for functional consequences of XAP2 binding to PDE2A we initially employed activity assays with purified proteins. Our results clearly show that XAP2 binding does not affect the enzymatic function of PDE2A. This finding is not trivial because the target segment of XAP2, i.e. the GAF-B domain, binds cGMP thereby enhancing PDE activity more than 20-fold. For instance, binding of XAP2 to PDE4A5 drastically reduced the catalytic activity of this isoform *in vitro* (25). Furthermore, XAP2 increased the sensitivity of PDE4A5 towards the inhibitor rolipram and attenuated the ability of cAMP-dependent protein kinase to phosphorylate PDE4A5 (25). Thus it appears that XAP2 may exert distinct effects on the various PDE isotypes. In line with this notion, we found that XAP2 targets PDE2A to the AhR complex, thereby inhibiting nuclear translocation of AhR. Association of XAP2 with transcription factors appears to be a rather general phenomenon, e.g. with hepatitis B virus protein X (9), Epstein-Barr virus encoded nuclear antigen 3 (29), thyroid hormone receptor (30) and of course AhR (12). One might envisage that XAP2-mediated targeting of PDE2A to AhR and possibly other transcription factors might be important for the spatially controlled regulation of cyclic nucleotide levels (31). Mutations in the XAP2 gene are known to predispose to pituitary adenoma formation (32) and therefore it is well conceivable that PDE2A and/or PDE4A5 might be involved in the pathogenesis of this disease. It will be important to test these intriguing possibilities.

Regulation of the AhR pathway by PDE2A

The AhR multiprotein complex consists of XAP2, a dimer of Hsp90, p23 and AhR (14,15). Binding of xenobiotics such as TCDD to AhR leads to the translocation of the ligand-bound receptor from the cytosol to the nucleus where it up-regulates the transcription of multiple genes for e.g. phase I drug metabolizing enzymes such as the CYP1 family, and phase II enzymes such as UGT1A1, GST-Ya subunit, and NADPH-quinone-oxido-reductase (33). Participation of

AhR in organ development, maturation of the immune system as well as cell proliferation, and differentiation (34) clearly implies that AhR can also operate in the absence of exogenous ligands. To date, the nature of endogenous signal(s) triggering AhR translocation is still obscure. Therefore it came as a surprise when cAMP was identified as a potent mediator of AhR intracellular trafficking, acting as a repressor rather than an activator of AhR-dependent gene expression (20). In line with this notion, we could clearly demonstrate the permissive effects of PDE2A on cAMP-dependent translocation of native AhR. For example, forskolin (an adenylyl cyclase activator) and 8-Br-cAMP (a membrane-permeating cAMP analog)-induced nuclear translocation of AhR were inhibited in cells expressing PDE2A. In addition, we observed a reduction of TCDD-induced gene expression by PDE2A.

Our finding that PDE2A may serve as a regulatory component of the AhR complex has important implications. For instance, PDE2A binding may ensure AhR retention in the cytoplasm, possibly by lowering the local cAMP concentrations under a level required for AhR complex translocation. Hence present efforts aim at the precise mechanisms underlying the effects of PDE2 on AhR translocation and complex formation. Yet another challenge is to unravel the molecular mechanisms mediating the effects of cAMP on AhR translocation. In this context it is worth mentioning that AhR is not phosphorylated by cAMP-dependent protein kinase *in vitro* (data not shown) even though protein kinase A inhibitor H89 can abolish the cAMP-induced nuclear effects of AhR (20). Clearly a deeper understanding of the cAMP-driven effects on the AhR pathway will help to elucidate the role of PDE2A in this intricate signaling network surrounding AhR.

ACKNOWLEDGEMENTS

We would like to thank Barbara Oesch-Bartlomowicz, Alvaro Puga and Gary H. Perdew for kindly providing us with cDNA constructs and cell lines, and all members of the Institute for Biochemistry II for help and discussions. S.K.O was funded by a scholarship from the Coordenação de Aperfeiçoamento de Pessoal de Nível Superior and the German Academic Exchange Service (CAPES/DAAD). S.G. was supported by grant WA366 and the work was supported by grant SFB553 both from the Deutsche Forschungsgemeinschaft.

REFERENCES

1. Iffland, A., Kohls, D., Low, S., Luan, J., Zhang, Y., Kothe, M., Cao, Q., Kamath, A. V., Ding, Y. H., and Ellenberger, T. (2005) *Biochemistry* **44**, 8312-8325
2. Soderling, S. H., and Beavo, J. A. (2000) *Curr Opin Cell Biol* **12**, 174-179
3. Rosman, G. J., Martins, T. J., Sonnenburg, W. K., Beavo, J. A., Ferguson, K., and Loughney, K. (1997) *Gene* **191**, 89-95
4. MacFarland, R. T., Zelus, B. D., and Beavo, J. A. (1991) *J Biol Chem* **266**, 136-142
5. Mongillo, M., Tocchetti, C. G., Terrin, A., Lissandron, V., Cheung, Y. F., Dostmann, W. R., Pozzan, T., Kass, D. A., Paolocci, N., Houslay, M. D., and Zaccolo, M. (2006) *Circ Res* **98**, 226-234
6. Seybold, J., Thomas, D., Witzenrath, M., Boral, S., Hocke, A. C., Burger, A., Hatzelmann, A., Tenor, H., Schudt, C., Krull, M., Schutte, H., Hippenstiel, S., and Suttorp, N. (2005) *Blood* **105**, 3569-3576
7. Martinez, S. E., Wu, A. Y., Glavas, N. A., Tang, X. B., Turley, S., Hol, W. G., and Beavo, J. A. (2002) *Proc Natl Acad Sci U S A* **99**, 13260-13265
8. Wu, A. Y., Tang, X. B., Martinez, S. E., Ikeda, K., and Beavo, J. A. (2004) *J Biol Chem* **279**, 37928-37938
9. Kuzhandaivelu, N., Cong, Y. S., Inouye, C., Yang, W. M., and Seto, E. (1996) *Nucleic Acids Res* **24**, 4741-4750
10. Carver, L. A., LaPres, J. J., Jain, S., Dunham, E. E., and Bradfield, C. A. (1998) *J Biol Chem* **273**, 33580-33587
11. Ma, Q., and Whitlock, J. P., Jr. (1997) *J Biol Chem* **272**, 8878-8884
12. Meyer, B. K., Pray-Grant, M. G., Vanden Heuvel, J. P., and Perdew, G. H. (1998) *Mol Cell Biol* **18**, 978-988
13. Lamb, J. R., Tugendreich, S., and Hieter, P. (1995) *Trends Biochem Sci* **20**, 257-259

14. Fujii-Kuriyama, Y., and Mimura, J. (2005) *Biochem Biophys Res Commun* **338**, 311-317
15. Marlowe, J. L., and Puga, A. (2005) *J Cell Biochem* **96**, 1174-1184
16. Bock, K. W., and Kohle, C. (2006) *Biochem Pharmacol* **72**, 393-404
17. Harper, P. A., Riddick, D. S., and Okey, A. B. (2006) *Biochem Pharmacol* **72**, 267-279
18. Denison, M. S., and Nagy, S. R. (2003) *Annu Rev Pharmacol Toxicol* **43**, 309-334
19. Ramadoss, P., Marcus, C., and Perdew, G. H. (2005) *Expert Opin Drug Metab Toxicol* **1**, 9-21
20. Oesch-Bartlomowicz, B., Huelster, A., Wiss, O., Antoniou-Lipfert, P., Dietrich, C., Arand, M., Weiss, C., Bockamp, E., and Oesch, F. (2005) *Proc Natl Acad Sci U S A* **102**, 9218-9223
21. Schultess, J., Danielewski, O., and Smolenski, A. P. (2005) *Blood* **105**, 3185-3192
22. Meurer, S., Pioch, S., Gross, S., and Muller-Esterl, W. (2005) *J Biol Chem* **280**, 33149-33156
23. Bentley, J. K., Juilfs, D. M., and Uhler, M. D. (2001) *J Neurochem* **76**, 1252-1263
24. Gross-Langenhoff, M., Hofbauer, K., Weber, J., Schultz, A., and Schultz, J. E. (2006) *J Biol Chem* **281**, 2841-2846
25. Bolger, G. B., Peden, A. H., Steele, M. R., MacKenzie, C., McEwan, D. G., Wallace, D. A., Huston, E., Baillie, G. S., and Houslay, M. D. (2003) *J Biol Chem* **278**, 33351-33363
26. D'Andrea, L. D., and Regan, L. (2003) *Trends Biochem Sci* **28**, 655-662
27. Bell, D. R., and Poland, A. (2000) *J Biol Chem* **275**, 36407-36414
28. Petrulis, J. R., Kusnadi, A., Ramadoss, P., Hollingshead, B., and Perdew, G. H. (2003) *J Biol Chem* **278**, 2677-2685
29. Kashuba, E. V., Gradin, K., Isaguliants, M., Szekely, L., Poellinger, L., Klein, G., and Kazlauskas, A. (2006) *J Biol Chem* **281**, 1215-1223
30. Froidevaux, M. S., Berg, P., Seugnet, I., Decherf, S., Becker, N., Sachs, L. M., Bilesimo, P., Nygard, M., Pongratz, I., and Demeneix, B. A. (2006) *EMBO Rep* **7**, 1035-1039
31. Zaccolo, M., Di Benedetto, G., Lissandron, V., Mancuso, L., Terrin, A., and Zamparo, I. (2006) *Biochem Soc Trans* **34**, 495-497
32. Vierimaa, O., Georgitsi, M., Lehtonen, R., Vahteristo, P., Kokko, A., Raitila, A., Tuppurainen, K., Ebeling, T. M., Salmela, P. I., Paschke, R., Gundogdu, S., De Menis, E., Makinen, M. J., Launonen, V., Karhu, A., and Aaltonen, L. A. (2006) *Science* **312**, 1228-1230
33. Ramadoss, P., and Perdew, G. H. (2005) *Biochemistry* **44**, 11148-11159
34. Carlson, D. B., and Perdew, G. H. (2002) *J Biochem Mol Toxicol* **16**, 317-325

FIGURE LEGENDS

Figure 1. PDE2A and XAP2 interact in pull-down and co-immunoprecipitation assays.
1A: Expression of XAP2 as GST fusion protein. XAP2, N-terminally fused to GST, and GST alone were purified from *E.coli* using GSH sepharose beads, subjected to SDS-PAGE and stained with Coomassie brilliant blue.
1B: Pull-down assay using either GST-XAP2 or GST. COS-1 cells were transfected with VSV-tagged PDE2A, 48 hours after transfection the cells were lysed (PDE2A input) and incubated with GST-XAP2 or GST, using the same amounts as shown in Fig. 1A, for 4 h at 4°C. The beads were washed 5x with lysis buffer before adding 3x SDS-buffer and boiling. Proteins were separated by SDS-PAGE, immunoblotted and stained with mouse anti-VSV followed by HRP-coupled secondary antibody and chemiluminescence detection. PDE2A migrates as a 110-kDa protein.
1C: Co-immunoprecipitation of PDE2A and XAP2. COS-1 cells were co-transfected with VSV-tagged PDE2A and FLAG-tagged XAP2. Cells were lysed 48 hours after transfection cells and XAP2 was immunoprecipitated with anti-FLAG M2 affinity gel for 2 h at 4°C. The immunoprecipitates were washed and analyzed by immunoblot using mouse anti-VSV antibody (upper panel). Likewise protein total cell lysates were separated by SDS-PAGE and immunoblotted (center and lower panels). Data are representative of at least five independent experiments.
1D: Co-immunoprecipitation of endogenous PDE2A and XAP2 from rat brain. Brain tissue was lysed and PDE2A or XAP2 proteins were precipitated using specific antibodies for 1 h at 4°C followed by protein A or G bound to sepharose beads for 1 h (IP). Precipitated proteins were solubilized, separated by SDS-PAGE and immunoblotted with PDE2A and XAP2 antibodies (IB). As control non-specific antibodies (IgG) were used. In the first lane expression of PDE2 and XAP2 in total brain lysate is shown. Data are representative of three independent experiments.

Figure 2. Co-localization of PDE2A and XAP2 in HeLa cells.
HeLa cells were co-transfected with myc-tagged XAP2 and VSV-tagged PDE2A. Cells were fixed 24 h after transfection, permeabilized and double-labeled with rabbit anti-myc and mouse anti-VSV followed by incubation with carbocyanine-conjugated secondary antibodies (Cy3-anti-rabbit and Cy2-anti-mouse). Cells were visualized by confocal microscopy. Panels A and B show stainings of myc-tagged XAP2 and VSV-tagged PDE2A alone, and panel C is the overlay of both pictures. Bar, 10 µm. The figure is representative of three independent experiments.

Figure 3. The GAF B domain of PDE2A interacts with XAP2.
3A: PDE2A constructs. The scheme shows the PDE2A domain organization and indicates the size of deletion constructs used for binding site mapping experiments (see below).
3B: Mapping of the XAP2 binding site of PDE2A. COS-1 cells were transfected with N-terminally VSV-tagged PDE2A deletion constructs (see above). Cell lysates were prepared 48 h after transfection (input) and incubated with GST-XAP2 or GST coupled to beads for 4 h at 4°C. Beads were washed 5x with lysis-buffer before adding SDS-buffer and boiling. Proteins were separated by SDS-PAGE and identified by immunoblotting with mouse anti-VSV. Shown data are repesentative of at least 3 independent experiments.

Figure 4. XAP2 binds PDE2A through its TPR domain.
4A: XAP2 constructs. The scheme shows the XAP2 domains and the amino- (N-XAP2) and carboxy-terminal (C-XAP2) constructs used for pull-down experiments (see below).
4B: Expression of XAP2 constructs. SDS-PAGE analysis of GST fusion proteins used in the pull-down assay, proteins were stained with Coomassie brilliant blue.
4C: Mapping of the PDE2A binding region of XAP2. COS-1 cells were transfected with VSV-tagged full-length PDE2A. Cells were lysed 48 h after transfection (PDE2A input) and incubated with GST-N-XAP2, GST-C-XAP2, GST-XAP2 or GST alone. Precipitated proteins were analyzed by SDS-PAGE and bound PDE2A was identified by immunoblotting with mouse anti-VSV. Data are representative of at least three independent experiments.

Figure 5: XAP2 does not interfere with PDE2A catalytic activity.
5A: Recombinant expression of PDE2A: COS-1 cells were transfected with a vector encoding VSV-tagged PDE2A. Two days after transfection cells were lysed, PDE2A was precipitated using anti-VSV and protein A agarose and analyzed by SDS-PAGE and Coomassie staining. PDE2A migrates at a size of about 110 kDa, the bands at 50 kDa and 25 kDa correspond to the heavy and light chain (hc and lc) of the antibody used for purification (anti-VSV). The figure is representative of three independent experiments.
5B: PDE activity assay: PDE2A purified from transfected COS-1 cells (5 µl, approximately 2.5 nM final concentration) bound to protein A agarose beads were incubated for 10 min at room temperature without or with 125 nM of each of the following GST derivatives: GST-XAP2, GST-N-XAP2, GST-C-XAP2 or GST alone. Then, 25 µM cAMP (final concentration) was added and the PDE reaction was carried out for 1 hour at 30°C. As controls anti-VSV/protein A agarose precipitates from mock transfected COS-1 cells (mock) and buffer alone (buffer) were analyzed. After that, SDS loading buffer was added to the reaction mixtures and the concentration of PDE2A was monitored by SDS-PAGE and immunoblotting with anti-VSV (inset). Error bars indicate standard deviation. Shown is one representative experiment performed in quintuplicate; two additional experiments with similar results were done in triplicate each.

Figure 6: Cellular localization of AhR in PDE2A transfected cells. Hepa1c1c7 cells were grown on glass coverslips for 48 h before transfection with VSV-tagged PDE2A. One day post-transfection cells were treated with 5 nM TCDD (D and E, F), 20 µM forskolin (G and H, I) or 2 mM 8-Br-cAMP (J and K, L) for 1 h at 37°C, fixed, permeabilized and stained with goat anti-AhR (M20) to visualize endogenous AhR and with mouse anti-VSV, to detect transfected PDE2A. This was followed by incubation with secondary antibodies (Cy3-anti-goat, Cy2-anti-mouse). PDE2A transfected cells are shown as merge of AhR (red) and PDE2A (green) stainings (B, E, H, K), or with the AhR staining alone (C, F, I, L). Untreated cells are presented as controls (A and B, C). Arrows point to cells that

exhibit a reduced nuclear AhR staining in the untreated state and to cells that have lost the capacity for AhR translocation under the respective treatment. Bar, 20 µm. The experiments are typical of one done at least three times.

Figure 7: PDE2A inhibits TCDD-induced gene transcription. Hepa1c1c7 cells grown on 96 well plates were transfected with pGL3-Basic empty vector (control) or p1646p1Luc3 (Cyp1a1), a reporter vector containing firefly luciferase under the control of the cytochrome P450 1A1 natural promoter, together with VSV-tagged PDE2A. To quantitate transfection levels the pRL-SV40 vector was co-transfected which expresses *Renilla* luciferase constitutively. One day posttransfection cells were treated with 5 nM TCDD for 4 h at 37°C, lysed, luciferase activities were determined and plotted as ratios of firefly versus *Renilla* luciferase activities in relative light units (RLU). Levels of transfected PDE were analyzed by immunoblotting with an antibody against the VSV-tag (PDE, shown below). Data shown are means ± S.E. of four independent experiments performed in quadruplicate; * indicates that the difference is statistically significant ($p < 0.02$, *t*-test).

Table 1: AhR translocation in Hepa1c1c7 cells.
Quantitative evaluation of AhR translocation induced by treatment with TCDD, forskolin or 8-Br-cAMP in untransfected Hepa1c1c7 cells and in cells expressing PDE2A. Cells were assigned into two groups dependent on the subcellular distribution of the AhR. The "spread" group comprises cells with cytosolic as well as nuclear staining of AhR, whereas the cells of the "nuclear" group had a predominant or exclusive nuclear AhR staining. n indicates the number of analyzed cells. Shown data are derived from at least three independent experiments.

	AhR localization in untransfected cells		
	spread	nuclear	% AhR translocation
untreated (n=202)	195	7	3.5
TCDD (n=207)	36	171	82.6
forskolin (n=187)	40	147	78.6
8-Br-cAMP (n=194)	38	156	80.4

	AhR localization in PDE2A transfected cells		
	spread	nuclear	% AhR translocation
untreated (n=174)	170	4	2.3
TCDD (n=177)	100	77	43.5
forskolin (n=119)	91	28	23.5
8-Br-cAMP (n=72)	59	13	18.0

Figure 1

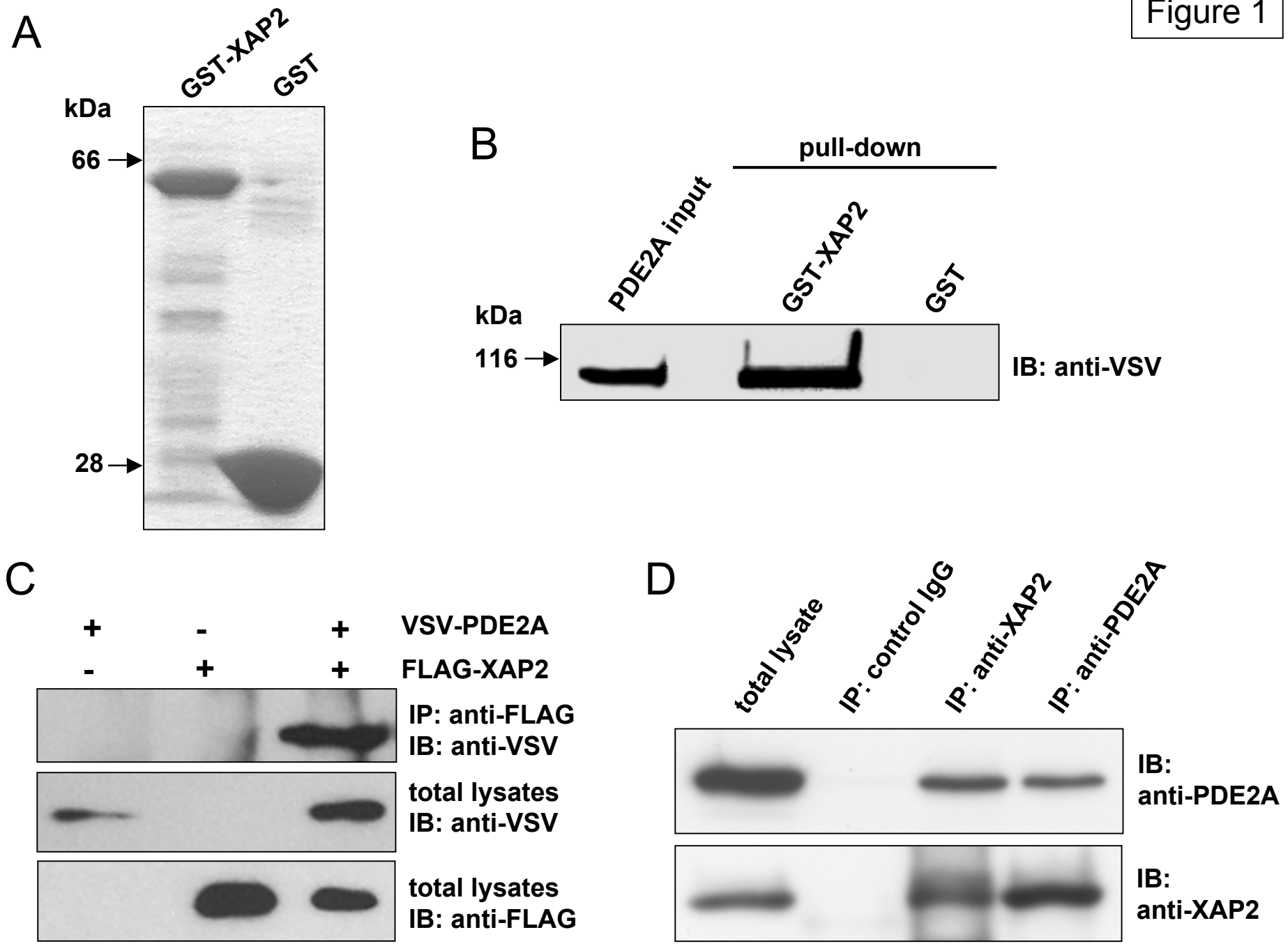
A
GST-XAP2
GST
kDa
66
28
B
pull-down
PDE2A input
GST-XAP2
GST
kDa
116
IB: anti-VSV
C
+
-
+
VSV-PDE2A
-
+
+
FLAG-XAP2
IP: anti-FLAG
IB: anti-VSV
total lysates
IB: anti-VSV
total lysates
IB: anti-FLAG
D
total lysate
IP: control IgG
IP: anti-XAP2
IP: anti-PDE2A
IB:
anti-PDE2A
IB:
anti-XAP2

Figure 2

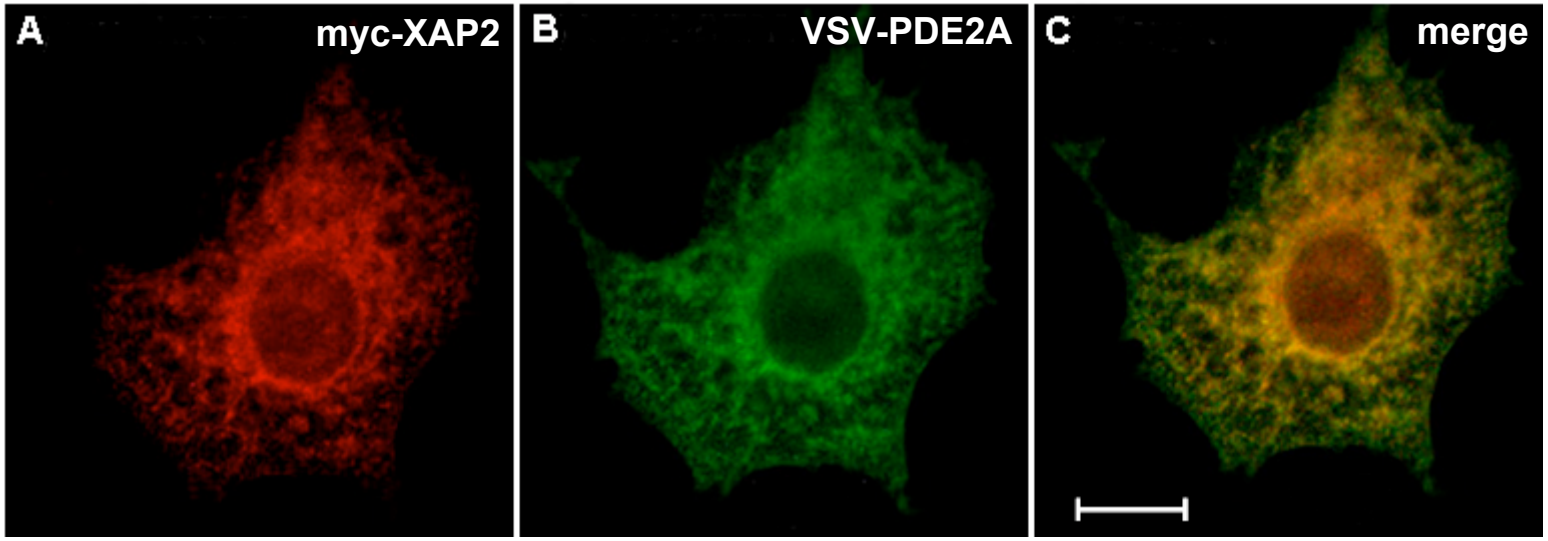

Figure 3

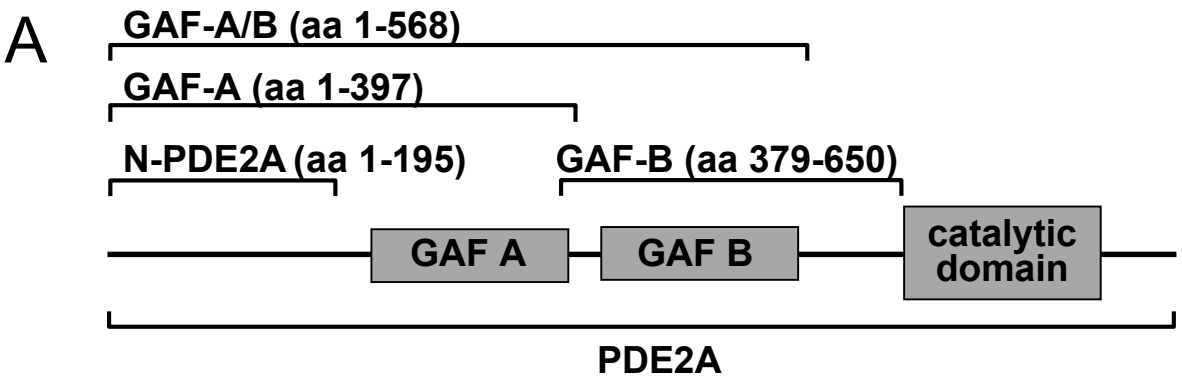
A
GAF-A/B (aa 1-568)
GAF-A (aa 1-397)
N-PDE2A (aa 1-195)
GAF-B (aa 379-650)
GAF A
GAF B
catalytic domain
PDE2A

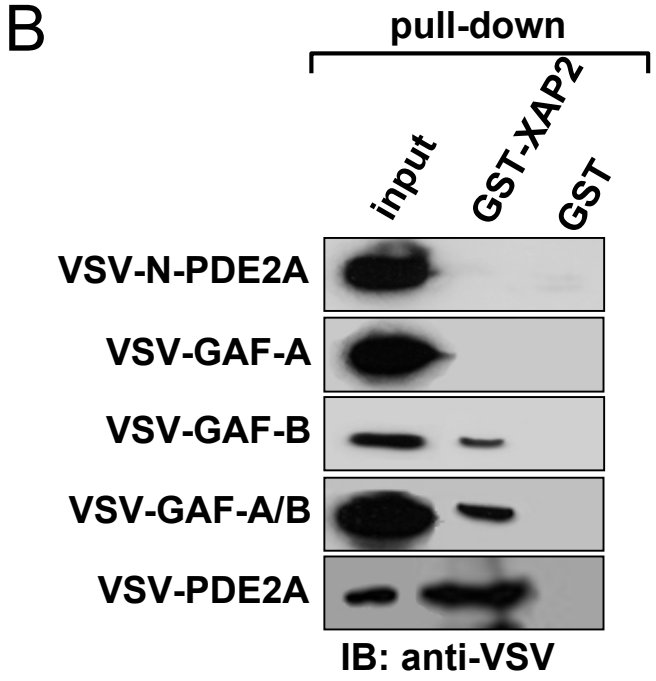
B
pull-down
input
GST-XAP2
GST
VSV-N-PDE2A
VSV-GAF-A
VSV-GAF-B
VSV-GAF-A/B
VSV-PDE2A
IB: anti-VSV

Figure 4

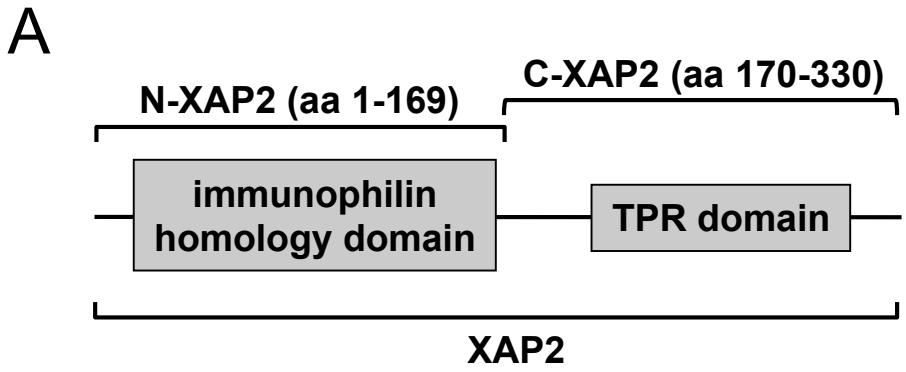
A
N-XAP2 (aa 1-169)
C-XAP2 (aa 170-330)
immunophilin homology domain
TPR domain
XAP2

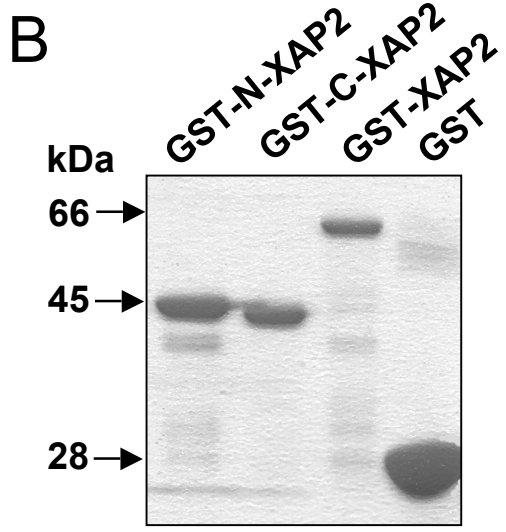
B
GST-N-XAP2
GST-C-XAP2
GST-XAP2
GST
kDa
66
45
28

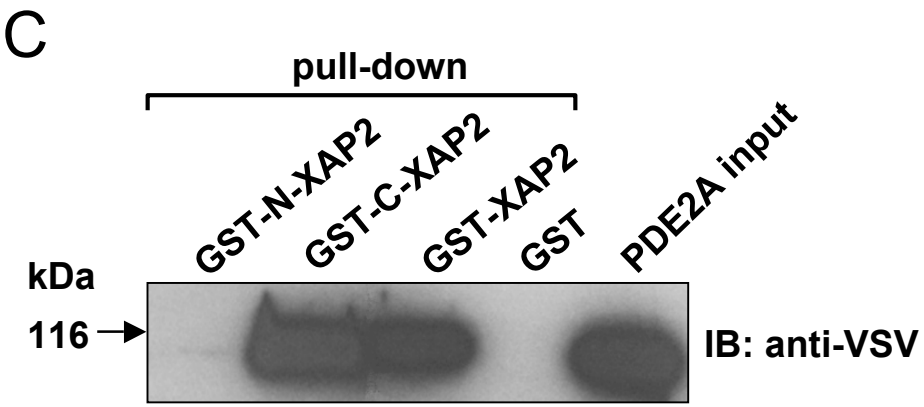
C
pull-down
GST-N-XAP2
GST-C-XAP2
GST-XAP2
GST
PDE2A input
kDa
116
IB: anti-VSV

Figure 5

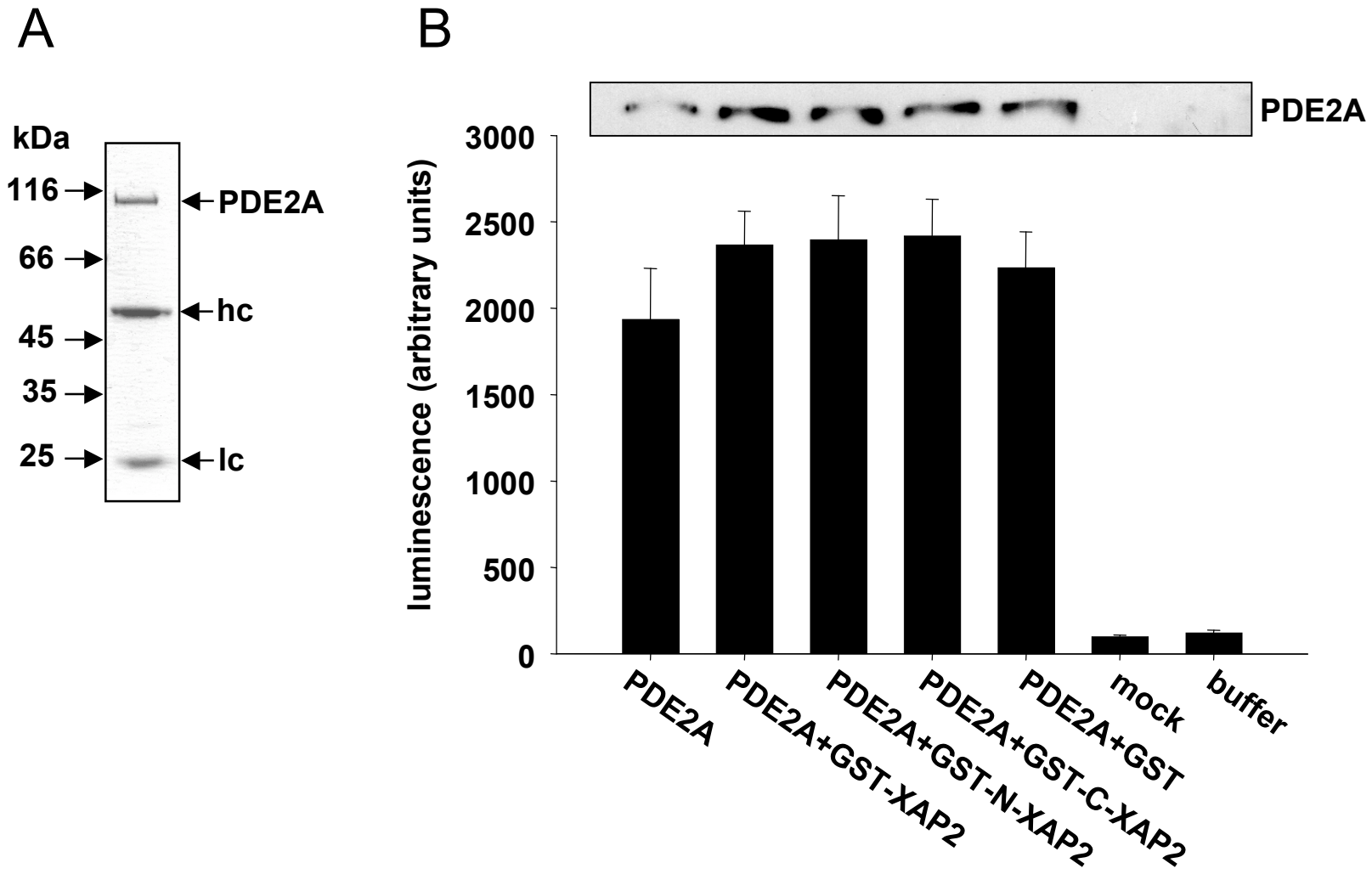
A
kDa
116
66
45
35
25
PDE2A
hc
lc
B
PDE2A
luminescence (arbitrary units)
3000
2500
2000
1500
1000
500
0
PDE2A
PDE2A+GST-XAP2
PDE2A+GST-N-XAP2
PDE2A+GST-C-XAP2
PDE2A+GST
mock
buffer

Figure 6

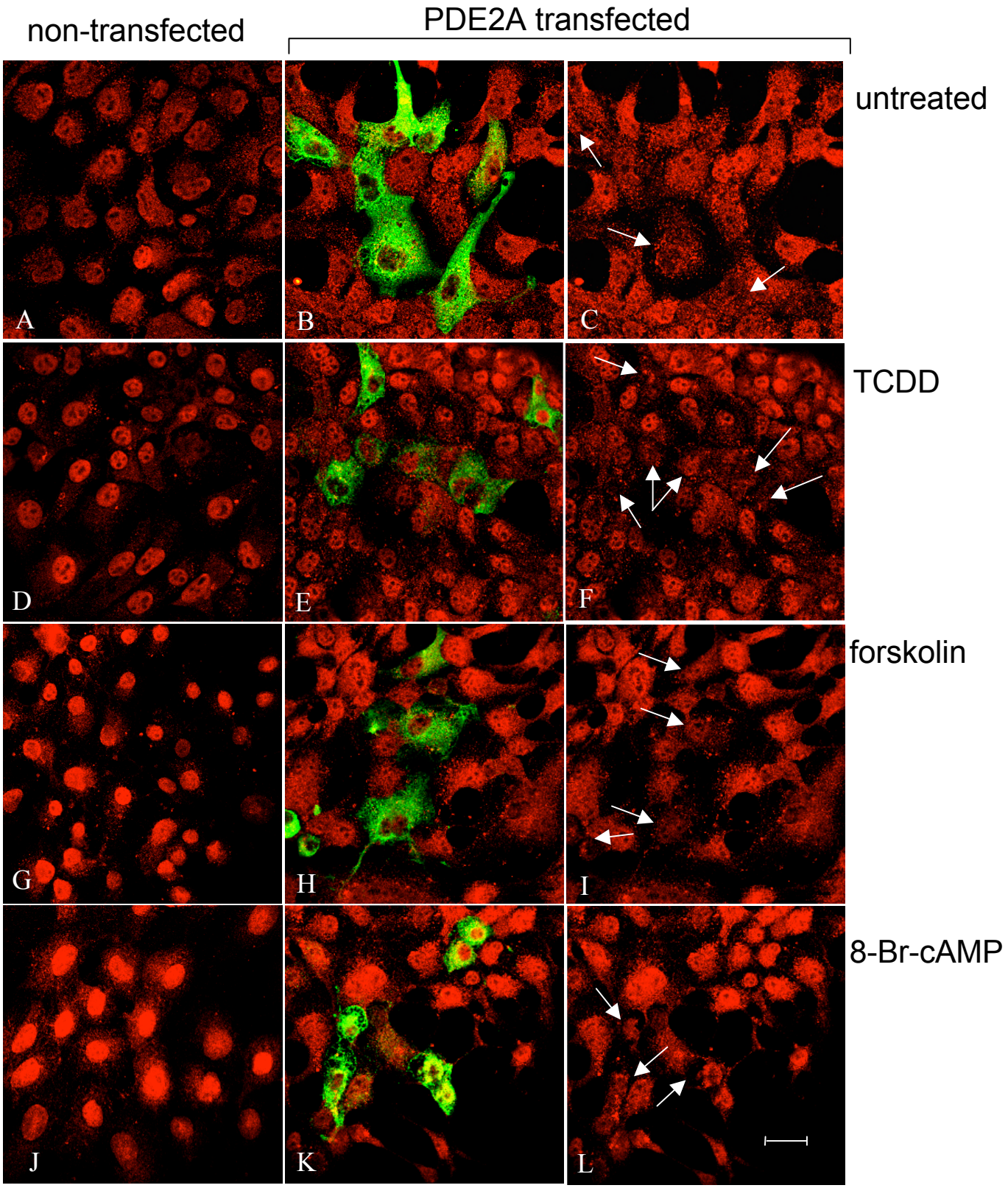
non-transfected
PDE2A transfected
untreated
TCDD
forskolin
8-Br-cAMP
A
B
C
D
E
F
G
H
I
J
K
L

Figure 7

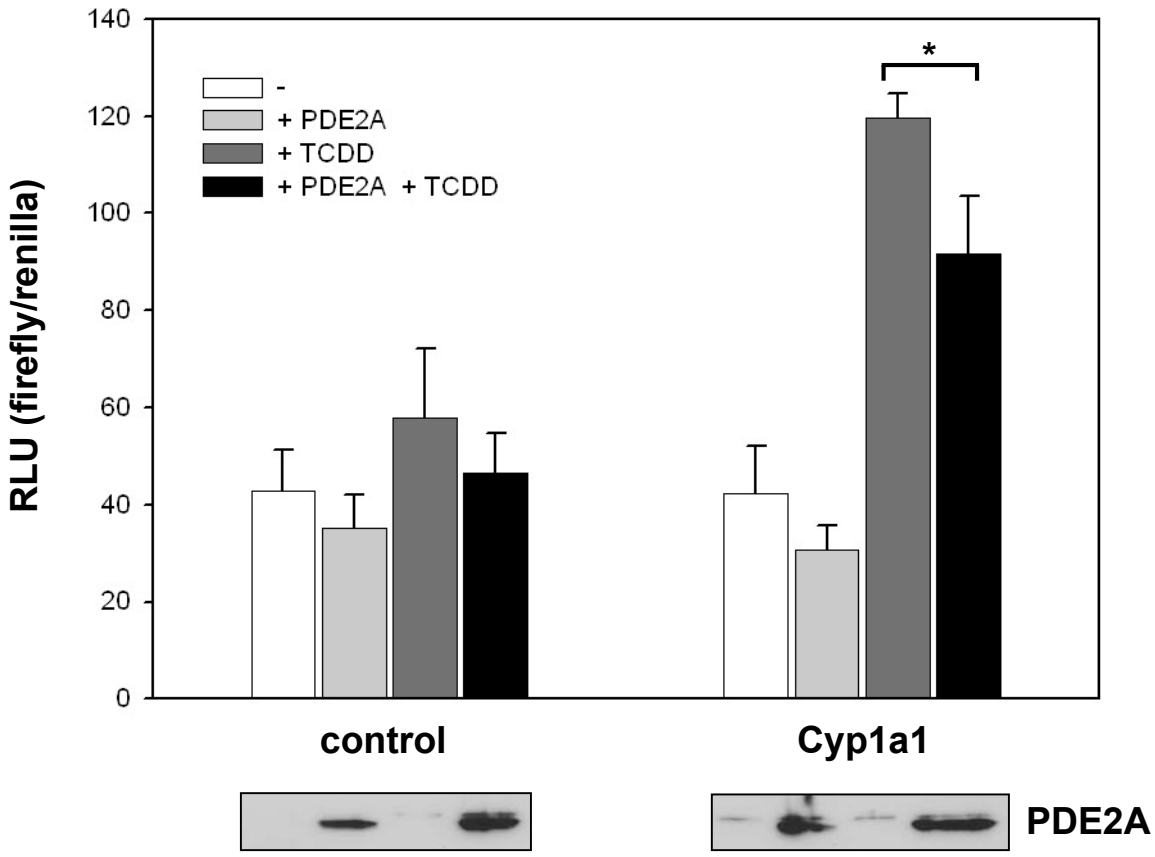
RLU (firefly/renilla)
140
120
100
80
60
40
20
0
-
+ PDE2A
+ TCDD
+ PDE2A + TCDD
*
control
Cyp1a1
PDE2A